Draft Jan. 11, 1999 To be submitted to J. Non-Cryst. Solids

^{6}Li, ^{7}Li nuclear magnetic resonance investigation of lithium coordination in binary phosphate glasses

Todd M. Alam[a*], Sam Conzone[b], Richard K. Brow[b], and Timothy J. Boyle[c],

[a] Sandia National Laboratories, Department of Aging and Reliability in Bulk Materials, Albuquerque, NM 87185-1407 USA.
[b] University of Missouri-Rolla, Ceramic Engineering Department, Rolla, MO 65409 USA
[c] Sandia National Laboratories, Materials Processing Department, Advanced Materials Laboratory, 1001 University Blvd. SE., Albuquerque, NM 87106 USA.

Abstract

^{6}Li and ^{7}Li solid state magic angle spinning (MAS) nuclear magnetic resonance (NMR) spectroscopy has been used to investigate the local coordination environment of lithium in a series of $x Li_2O \cdot (1-x)P_2O_5$ glasses, where $0.05 \leq x \leq 0.55$. Both the ^{6}Li and ^{7}Li show chemical shift variations with changes in the Li_2O concentration, but the observed ^{6}Li NMR chemical shifts closely approximate the true isotropic chemical shift and can provide a measure of the lithium bonding environment. The ^{6}Li NMR results indicate that in this series of lithium phosphate glasses the Li atoms have an average coordination between four and five. The results for the metaphosphate glass agree with the coordination number and range of chemical shifts observed for crystalline $LiPO_3$. An increase in the ^{6}Li NMR chemical shift with increasing Li_2O content was observed for the entire concentration range investigated, correlating with increased cross-linking of the phosphate tetrahedral network by O-Li-O bridges. The ^{6}Li chemical shifts were also observed to vary monotonically through the anomalous glass transition temperature (T_g) minimum. This continuous chemical shift variation shows that abrupt changes in the Li coordination environment do not occur as the Li_2O concentration is increased, and such abrupt changes can not be used to explain the T_g minimum.

Keywords: ^{6}Li, ^{7}Li nuclear magnetic resonance; magic angle spinning; chemical shift; coordination number; glasses; ultraphosphate glasses; alkali glasses

* Corresponding author. Tel. +1 505 844 1225; fax +1 505 844 9624; e-mail: tmalam@sandia.gov.

DISCLAIMER

1. Introduction

Phosphate glasses have proven to be technologically important materials for a variety of applications including glass-to-metal seals, waste form encapsulants, biomedical components, fast ion conducters, glass-ceramic cation exchangers and optical devices.[1-8] Understanding the relationship between the structure of a material and the resulting physical properties is crucial for the rational design, optimization and modification of future materials. Unfortunately, the accurate and reliable prediction of physical properties in glasses, including the common glass transition temperature (T_g) in oxide glasses, remains difficult due to the lack of detailed structural information.[9] For example, in binary alkali ultraphosphate glasses, $x Li_2O \cdot (1-x)P_2O_5$ ($x < 0.5$ mole fraction alkali), a minimum in T_g is observed near the $x = 0.2$ M_2O (M = Li, Na) modifier concentration.[10,11] Figure 1 shows the T_g behavior for the $x Li_2O \cdot (1-x)P_2O_5$ glasses as function of Li_2O concentration.[10,11] Similar reductions in the T_g have been noted in silicate glasses with increasing alkali content, but the "anomalous" increasing T_g behavior has not been previously reported. The decrease in the T_g has been attributed to the loss of the fully polymerized Q^3 phosphate tetrahedral network (where in the Q^n nomenclature, n refers to the number of bridging oxygens (BO) per phosphorous).[10,11] The increase in the T_g above $x \sim 0.2$ mole fraction is consistent with some restructuring or medium range ordering (MRO) that occurs in the glass structure, including an increase of alkali-nonbridging oxygen (NBO) interactions.

The structural mechanism for these anomalous effects in the alkali ultraphosphate glass system has yet to be determined. Therefore, a variety of investigations have been performed to try to provide experimental evidence for the structural basis of the anomalous T_g behavior in ultraphosphate glasses, including nuclear magnetic resonance (NMR) spectroscopy investigations.[9,12-14] The local structure of the phosphate tetrahedra has been studied in detail using ^{31}P NMR.[15,16] Two-dimensional dipolar recoupled exchange and double quantum ^{31}P NMR experiments have recently been used to investigate the connectivity between different Q^n species within alkali ultraphosphate glasses.[9,17,18] Investigations of the alkali modifiers, in particular ^{23}Na NMR, have also addressed the question of the coordination environment in phosphate glasses. In a Li, Na

mixed alkali metaphosphate series of glasses, increases in the [Na]/[Na+Li] ratio produced an increased in the ^{23}Na chemical shift (becoming more deshielded),[19] due to the presence of Li-NBO-Na bonding. Second moment (M_2) analysis of the wide-line ^{7}Li spectra in phosphate glasses have also been used to demonstrate that there is a random distribution of lithium nuclei within the glass.[20]

Detailed information about the local coordination environment of Li in Li-phosphate crystals and glasses is limited. The Li coordination environment for the lithium metaphosphate ($LiPO_3$) glass has only recently being reported,[21] but additional structural studies of alkali ultraphosphate glasses are still lacking. The limited number of X-ray investigations of these glasses may result from the low scattering coefficient of Li, which prevents accurate determinations of atomic positions in X-ray diffraction studies. This difficulty is further compounded by the high degree of disorder commonly present in both crystals and glasses containing lithium. In this paper we report ^{6}Li and ^{7}Li solid state MAS NMR data obtained from selected lithium phosphate crystals and lithium ultraphosphate glasses.[22] The results of these NMR investigations provide details about the local Li coordination environment, and allow correlations between observed Li chemical shifts and structure properties of Li-ultraphosphate glasses to be developed. This simple, binary Li-ultraphosphate glass system should provide information about the structural components responsible for the anamolous T_g behavior in the alkali ultraphosphate glasses.

2. Experimental

The ^{6}Li and ^{7}Li MAS NMR spectra were acquired on a Bruker AMX-400 widebore spectrometer operating at 58.9 and 155.5 MHz, respectively. A 4mm broadband MAS probe allowed spinning speeds of 10 kHz to be used for all samples. Spectra were acquired using 1-2 μs pulses where the $\pi/2$ pulse length was determined to be 5 μs for ^{6}Li and 3 μs for ^{7}Li. Spectra were obtained using 64 through 4096 signal averages. For the $x Li_2O \cdot (1-x) P_2O_5$ glasses recycle delays were 10 seconds, while the crystalline compounds required from 10 to 480 seconds to reduce signal saturation. External 1M aqueous LiCl (δ = 0.00 ppm) was used as reference for both ^{6}Li and ^{7}Li. Labeled $^{6}LiCl$ (Isotech - 98 %) was used to prepare the ^{6}Li standard. The accuracy of the reported chemical shifts were

±0.2 ppm for ^{7}Li and ±0.05 ppm for ^{6}Li, as determined by repeated experiments and calibrations.

Of the five crystalline lithium phosphate materials analyzed by ^{6}Li and ^{7}Li MAS NMR, two were commercial preparations and three were synthetically prepared. Crystalline $LiPO_3$ (Alfa Æsar) and LiH_2PO_4 (Aldrich) were obtained commercially and used without further purification. Crystalline $Li_4P_2O_7$ and the high temperature (HT) form of Li_3PO_4 were prepared by dissolving the appropriate amounts of LiOH and phosphoric acid (~1ml) in an aqueous solution. Each solution was then dried overnight in an oven at 125°C to produce a white powder. This powder was subsequently melted on platinum foil at 900°C and 1200°C to generate Li_3PO_4 (HT) and $Li_4P_2O_7$, respectively. The melts were quenched by rapid cooling and then reheated at a rate of 3°C/min to a temperature of 450°C, where they were held for 1 hour to yield single-phase crystalline materials. The low temperature (LT) crystalline form of Li_3PO_4 was produced by slowly adding phosphoric acid to a boiling solution of LiOH and H_2O.[23] Crystals immediately precipitated as the phosphoric acid was added. The boiling mixture of crystals and water was stirred for ~ 5 minutes and then oven-dried overnight at 125°C. Both powder x-ray diffraction (XRD) and ^{31}P MAS NMR were used to confirm the phase purity of these crystalline compounds.

Lithium phosphate glasses ($xLi_2O{\cdot}(1\text{-}x)P_2O_5$, $x< 0.55$ mole fraction) were prepared using a slight modification to the sealed ampule technique described by Hudgens et. al.[10] Appropriate amounts of sublimation-dried P_2O_5 and lithium metaphosphate (50 mol% Li_2O, 50 mol% P_2O_5) glass powders were mixed in a drybox and placed in fused silica ampules. Each ampule was flame sealed under vacuum and the contents were melted at 900°C for ~ 1hr, after which the ampule was transferred to an inert atmosphere. All materials were stored and handled under argon to avoid water contamination of the glass. Differential scanning calorimetry (DSC) was used to determine the T_g of each glass in flowing argon, using a 10 °C/min scan after cooling from above T_g in the calorimeter at - 10 °C/min. Experimental T_g values were in agreement with those previously published for lithium ultraphosphate glasses.[11]

3. Results

The ^{7}Li and ^{6}Li solid state MAS NMR spectra for low temperature (LT) form of Li_3PO_4 are shown in Figure 2, and are representative of the NMR spectra obtained for the lithium phosphate crystals investigated. For the ^{7}Li ($I = 3/2$) spectrum (Fig. 2a) a strong central resonance is observed, resulting from the $\pm 1/2 \leftrightarrow \mp 1/2$ transition, along with the spinning sideband manifold due to the $\pm 3/2 \leftrightarrow \pm 1/2$ transitions. For ^{6}Li ($I = 1$) (Fig. 2b) only a single resonance is observed, resulting from the $0 \leftrightarrow \pm 1$ transitions. Simulation of these line shapes allowed the determination of the observed chemical shift and full width at half maximum line widths (FWHM) for the investigated phosphate crystals (Table 1). The magnitude of the electrical quadrupolar coupling constant (C_Q) for the ^{7}Li nuclei can also be estimated from the range spanned by the spinning sideband manifold in the MAS spectra and are given in Table 1. Multiple overlapping isotropic resonances were observed in the ^{6}Li NMR spectra of crystalline $LiPO_3$ and $Li_4P_2O_7$, and result from inequivalent Li environments in these crystals. The experimental and the corresponding simulated spectra for crystalline $Li_4P_2O_7$ and $LiPO_3$ are shown in Figure 3a and Figure 3b, respectively. The isotropic chemical shift and FWHM of these deconvoluted resonances are given in Table 1. It is interesting to note that in the ^{7}Li NMR spectra of these crystals, the inequivalent Li environments could not be resolved, and thus only a single broad resonance was observed.

Representative ^{7}Li and ^{6}Li solid state MAS NMR spectra for the series of lithium phosphate $xLi_2O \cdot (1\text{-}x)P_2O_5$ glasses are shown in Figure 4 ($x = 0.5$). For all of the glasses investigated only a single broad central transition in the ^{7}Li NMR spectra and a single broad isotropic resonance in the ^{6}Li NMR spectra were observed. The observed chemical shifts, FWHM, C_Q and estimated errors are given in Table 2. Figure 5 provides a graphical representation of the variation of the ^{6}Li chemical shift (5a) and FWHM (5b) as a function of Li_2O concentration. A gradual decrease in both the ^{7}Li and ^{6}Li chemical shift with decreasing Li_2O concentration is observed. The variation of the ^{6}Li and ^{7}Li FWHM and C_Q with changing Li_2O concentration prove more variable and are discussed below. Due to the quadrupolar interaction (*vide infra*) the observed ^{6}Li parameters will provide the basis of later discussions of the local Li coordination environment.

Because ^{7}Li and ^{6}Li are both quadrupolar nuclei, the influence of the quadrupolar interaction must be determined in order to obtain true chemical shift information. For ^{7}Li ($I = 3/2$) the first order quadrupolar interaction has no effect on the $\pm 1/2 \leftrightarrow \mp 1/2$ central transition. Second order quadrupolar interaction may influence this transition, but no *anisotropic* second order quadrupolar broadening is observed for any of the lithium ultraphosphates glasses. An *isotropic* second order quadrupolar induced shift may be present and requires evaluation. In the presence of an isotropic second order quadrupolar shift the observed chemical shift in the MAS spectra is given by the sum of the true isotropic chemical shift and the isotropic second order quadrupolar chemical shift

$$\delta^{obs} = \delta^{CS} + \delta_{iso}^{(2Q)}. \tag{1}$$

For the $(m-1) \leftrightarrow m$ transition the isotropic second order quadrupolar shift (in ppm) is given by

$$\delta_{iso}^{(2Q)} = -\frac{3}{40}\frac{C_Q^2}{\nu_L^2}\frac{(I(I+1)-3-9m(m-1))}{I^2(2I-1)^2}\left(1+\frac{\eta_Q^2}{3}\right)\times 10^6 \tag{2}$$

where C_Q ($= e^2qQ/h$) is the quadrupolar coupling constant, η_Q is the quadrupolar asymmetry parameter, I spin quantum number and ν_L is the Larmor frequency. For ^{6}Li ($I = 1$) the isotropic first order quadrupolar chemical shift is zero, while the second order isotropic quadrupolar chemical shift is given by Eq. 2. Because the quadrupolar moment of ^{6}Li (-8.2×10^{-4} Q/10^{-28} m^2) is ~50 times smaller than ^{7}Li (-4.0×10^{-2} Q/10^{-28} m^2),[24] the isotropic second-order quadrupolar chemical shifts for ^{6}Li are considered negligible.[25] This allows the observed ^{6}Li chemical shift to accurately represent the true isotropic chemical shift. The difference between the ^{7}Li and ^{6}Li chemical shift can also be used to determine the magnitude of the quadrupolar coupling using a single magnetic field strength, through use of Eqs. 1 and 2. For the lithium phosphate crystals and glasses reported in Table 1 the shift differences at a magnetic field strength of 9.4 Tesla were very small (< 0.1 ppm, which approaches the resolution limit due to line

width) providing an upper limit of ~ 0.5 MHz for the quadrupolar coupling constant. The isotropic quadrupolar chemical shift appears to be slightly larger in the crystals than in the glasses, but as noted above individual ^{7}Li resonances were not resolved for the $Li_4P_2O_7$ and $LiPO_3$ crystals making this difficult to quantify. A more accurate estimate of C_Q as a function of Li modifier concentration could be obtained from the inverse proportionality of the quadrupolar shift to ν_L^2, but are not pursued here. For the discussion of chemical shift trends in the lithium phosphate systems presented below, the ^{6}Li NMR chemical shifts will be utilized almost exclusively.

4. Discussion

A correlation between the ^{6}Li NMR chemical shift and lithium coordination number (CN) was previously reported for lithium silicate and lithium aluminosilicate crystals and glasses.[25] In those lithium silicate systems, increasing CN (and accordingly increased Li-O bond distances) produced a decreased chemical shift (upfield shift, increased shielding, decreasing frequency) of ~ 0.6 ppm per each oxygen added to the Li coordination sphere. For example, lithium nuclei with CN = 6 were found to have ^{6}Li chemical shifts ranging from $\delta \sim$ –0.35 to -1.2 ppm, while lithium with CN = 4 were observed to have chemical shifts ranging from $\delta \sim$ +0.9 to +0.1 ppm. The decreasing chemical shift (increased shielding) is commonly explained by an increase in the Li-O ionicity with increasing average Li-O bond length that accompany higher coordination number. In ionic systems it has been argued that a decrease in the chemical shift results from the closed shell diamagnetic term of the chemical shielding. Increases in the chemical shift due to the increased covalent nature of the Li-O bond results from the paramagnetic term of the shielding tensor and involves the angular momentum of the excited bonding orbitals.[26-29] Similar trends in chemical shift with coordination number have been established for ^{29}Si, ^{23}Na, ^{27}Al and ^{25}Mg.[30-32] Previous investigations have also demonstrated that chemical shift correlations can be a very complex function involving a variety of structural parameters including CN, bond length, bond angle and counter ion identity. In many instances, the chemical shift ranges for different CN overlap, suggesting that other factors play an important role in determining

the observed chemical shift. For example, ^{23}Na NMR investigations of silicate and aluminosilicate crystals and melts have shown that decreases in the degree of network polymerization within the structure produce an increase in the ^{23}Na chemical shift.[31]

4.1 *Lithium phosphate crystals*

To investigate whether similar trends and correlations between chemical shift and local structure could be observed in lithium phosphate systems, the ^{6}Li NMR chemical shifts of select crystals were investigated and are reported in Table 1. The CN for the different lithium environments as determined from X-ray crystal investigations are also given in Table 1. For the low temperature (LT) form of Li_3PO_4, the crystal structure shows two distinct lithium sites in the Pmn21 unit cell.[23] Both inequivalent lithium nuclei have CN = 4, with average Li-O distances of 1.95 and 2.00 Å, respectively. The next nearest oxygen in the second coordination sphere is 2.87 Å. The two inequivalent lithium sites were not resolvable by ^{6}Li NMR, with the spectrum showing only a single resonance at δ = 0.32 ppm (Figure 2b). Similarly, the high temperature (HT) form of Li_3PO_4 has 2 distinct lithium sites in the Pmnb unit cell, with CN = 4, and average Li-O bond distances of 1.95 and 1.98 Å.[33] The distance to the next nearest oxygen in the second coordination sphere is 2.96 Å. Again only a single ^{6}Li NMR resonance was observed at δ = 0.36 ppm (Table 1). For both the HT and LT form of Li_3PO_4, the ^{6}Li NMR chemical shifts are consistent with the chemical shift ranges exhibited by tetrahedrally coordinated lithium in silicate crystals and glasses as reported by Xu and Stebbins.[25]

For crystalline LiH_2PO_4 ($Pna2_1$ unit cell) there is only one lithium environment, with CN = 4, and an average Li-O bond distance of 1.96 Å. The distance to the oxygen in the second coordination sphere is 3.25 Å. Only a single ^{6}Li NMR resonance was observed at δ = -0.26 ppm. For crystalline $Li_4P_2O_7$, there are 4 distinct Li sites in the $P_{2/m}$ unit cell.[34] All four of the lithium environments show a CN = 4, with Li-O bond distances ranging from 1.84 to 2.06 Å. The average Li-O bond distances for the four inequivalent sites are 1.95 and 1.97 (x3) Å (where x*n* denotes *n* number of Li sites having this distance). The next nearest oxygen distance in the second coordination sphere is ~ 3.15 Å. The signal from these four inequivalent Li environments produces a very broad ^{6}Li

NMR spectra (Figure 3a), which was deconvoluted into two resonances with isotropic chemical shifts of δ = -0.23 and -0.78 ppm. The observed chemical shifts of the tetrahedrally coordinated lithium in both crystalline LiH_2PO_4 and $Li_4P_2O_7$ are clearly outside the chemical shift range observed for CN = 4 in lithium silicate systems.[25]

For the metaphosphate $LiPO_3$ crystal there are 10 inequivalent lithium environments within the Pn unit cell.[35] All of the lithium species are reported to have CN = 4 with average Li-O distances of 1.93 (x3), 1.95 (x2), 1.96, 1.98 (x2), 1.99, and 2.00Å. The next nearest oxygen in the second sphere coordination for all ten lithium sites is ~ 2.9 to 3.0 Å. The ^{6}Li NMR spectrum of crystalline $LiPO_3$ (Figure 3b) is clearly composed of several overlapping resonances. This spectrum was deconvoluted into four different components with isotropic chemical shifts at δ = 0.16 (~20%), -0.14 (~10%), -0.43 (~40%) and –1.15 (~30%) ppm. As with $Li_4P_2O_7$, the observation of several upfield resonances (δ < 0 ppm) in $LiPO_3$ for lithium environments with CN = 4 *is inconsistent* with the simple relationship between chemical shift and CN presented by Xu and Stebbins.[25] It is interesting to note that in $LiPO_3$ a wide range of chemical shifts are observed while the average Li-O bond length varies over the small range of 1.93 to 2.0 Å, compared to a single resolvable resonance in Li_3PO_4 where the average Li-O bond length also varies from 1.95 to 2.0 Å.

One argument that might account for the observed range of chemical shifts is that the definition of coordination number in lithium systems is somewhat arbitrary. There are no distinct Li-O bond distance cutoffs that are used to define the first coordination sphere. Furthermore the increased disorder and low scattering coefficient of Li could make the accurate assignment of the Li coordination environment by diffraction techniques difficult. Xu and Stebbins re-evaluated the Li-O bond distances in LiO_n polyhedra in crystalline silicate and aluminosilicates and proposed Li-O bond lengths of 1.873, 1.979, 2.062, 2.219 and 2.235 Å for LiO_3, LiO_4, LiO_5, LiO_6 and LiO_8 polyhedra, respectively. For the lithium phosphate crystals reported in Table 1, there are no highly distorted coordination environments, and the observed bond distances fall within very defined ranges arguing that the assignment of CN = 4 for all the lithium sites is correct. For example, the reported bond distances observed in $LiPO_3$ are consistent with the LiO_4 polyhedra bond distances listed above, and the next nearest Li-O bond length of ~ 2.9 –

3.0 Å is much larger than the mean 2.235 Å listed for LiO_8 polyhedron.[35] From these data it is clear that the ^{6}Li NMR results for the $Li_4P_2O_7$ and $LiPO_3$ crystals demonstrate that the simple correlation between ^{6}Li chemical shift and CN previously presented is incomplete, and that other factors controlling chemical shift need to be considered.

In investigations of ^{23}Na NMR chemical shifts in silicates and alumino-silicates,[31] the degree of polymerization of the silicate network structure was found to correlate with the alkali chemical shift. In the silicate species the ^{23}Na chemical shift increased with increasing average number of NBO per tetrahedrally coordinated cation. A similar comparison can be made for the ^{6}Li chemical shifts in the lithium phosphate crystals investigated here. The number of NBO per phosphate tetrahedron (NBO/P)[36] can be related to the concentration of individual Q^n species (where n defines the number of bridging oxygens in a phosphate tetrahedra) and is given by

$$NBO/P = 4f(Q^0) + 3f(Q^1) + 2f(Q^2) + f(Q^3) \quad (3)$$

where $f(Q^n)$ is the site fractions of the different phosphate Q^n polyhedron types. The $f(Q^n)$ can easily be determined from the mole fraction of Li_2O added, as previously described.[13,17] In Eqn 3, it is assumed that the terminal oxygen (P=O) on the fully polymerized Q^3 phosphate tetrahedron is "non-bridging". Due to this terminal oxygen, the NBO/P ratio approaches unity in the fully polymerized P_2O_5 structure (pure Q^3), which contrasts to the limiting case of zero NBO per silicon in fully polymerized silicate systems. The ^{6}Li chemical shift versus the average NBO/P ratio for the lithium phosphate crystals is shown in Figure 6. Considerable scatter in the chemical shift for a given NBO/P ratio is observed for these lithium phosphate crystals. In particular the metaphosphate $LiPO_3$ crystal (NBO/P = 2) displays four different chemical shifts (Fig. 3b). For those crystals ($Li_4P_2O_7$ and $LiPO_3$) in which different Li chemical shifts were resolved, a weighted-average chemical shift was also determined, and is shown Figure 6 (filled symbols). There is a small, gradual increase in the weighted-average chemical shift with increasing NBO/P ratio, but there is still scatter at higher NBO/P values. This scatter in the relationship between NBO/P and the ^{6}Li NMR chemical shift suggest that the observed chemical shift can't be simply related to the average degree of polymerization,

and in general must be a complex function of bonding interactions with neighboring atoms.

One example of bonding interactions that may impact the observed ^{6}Li chemical shift is the charge distribution in the lithium-oxygen environment, requiring a measure of the oxygen chemical environment to correctly interpret the observed chemical shift behavior. Previous ^{23}Na NMR investigations [32] have shown that the ^{23}Na chemical shift correlates directly with the bond valence of the coordinating oxygens. Here we evaluated whether the same approach can be applied to the ^{6}Li chemical shifts in lithium phosphate systems. An empirical bond valence (s_{ij}) between an oxygen i and a cation j can be calculated from the oxygen-cation bond length r_{ij} (in Å) using[37-39]

$$s_{ij} = \exp[(r_0 - r_{ij}) / B)] \tag{4}$$

where r_0 is the empirically derived oxygen-cation bond length of unit valence, and B = 0.37 is a constant.[37-39] For the lithium phosphate system reported here, r_0 values of 1.466 Å for Li-O [37,38], 1.604 Å for P-O [37] and 0.95 Å for H-O [37] were utilized. The total atomic valence of the ith oxygen (W_i) is obtained from the sum over all oxygen-cation bond valences s_{ij} for each of the j cations bonded to the oxygen, including the lithium cations:

$$W_i = \sum_j s_{ij} \tag{5}$$

The chemical shift of the lithium is expected to correlate with the summation of the shift contributions of all oxygens located in a sphere 3-4 Å around Li through the oxygen bond valency and scaled by the lithium-oxygen bond distances r_i. A chemical shift parameter A has been defined by Koller et al. [32] and assumes a $1/r_i^3$ distance dependence

$$A = \sum_i \frac{W_i}{r_i^3} \tag{6}$$

The A shift parameters for the lithium phosphate crystals utilizing distances < 3.5 Å were calculated and are given in Table 1. The results of the correlation between A and experimental ^{6}Li chemical shifts is illustrated in Figure 7. A very good linear correlation (r = 0.95) was observed with

$$\delta_{cs}(^6\mathrm{Li}) = +4.30A - 5.85 \quad (7)$$

This linear correlation has a positive slope, which contrast to the negative slope reported for the ^{23}Na chemical shift versus A correlation.[32] To test the robustness of this correlation in other lithium compounds, chemical shift A values were also determined from the lithium neosilicate (Li_4SiO_4) crystal structure,[40] and compared to the ^{6}Li chemical shift reported by Xu and Stebbins.[25,41] A range of average chemical shift A values were determined for different LiO_n coordinations; LiO_6 have $\langle A \rangle \sim 1.05$, LiO_5 have $\langle A \rangle \sim 1.18$, LiO_4 have $\langle A \rangle \sim 1.27$ and the distorted LiO_4 (or LiO_3) have $\langle A \rangle \sim 1.34$. Utilizing these A values a linear correlation (r = 0.99) was also observed for Li_4SiO_4 (see Figure 7) and is given by

$$\delta_{cs}(^6\mathrm{Li}) = +7.50A - 8.52 \quad (8)$$

Several important observations were discerned from inspection of Figure 7. First a positive slope in the chemical shift versus A correlation was also observed for the different Li environments in Li_4SiO_4, but is ~2 times larger than observed in lithium phosphate crystals. It should be noted that the slope of this correlation is dependent on the assumptions made in assigning A values to given chemical shift in the lithium neosilicate. These assignments were chosen to maintain consistency with the chemical shift peak assignments based on coordination number originally proposed by Xu and Stebbins,[25] with the LiO_6 environment having the most negative chemical shift, while the LiO_3 lithium environments has the largest or most positive chemical shift.

The second observation is that the ^{6}Li chemical shift versus A correlation is different for these two different types of materials. These results demonstrate that the

chemical shift *A* formalism (Eqn 6) is still incomplete in fully describing the observed ^{6}Li chemical shifts for lithium phosphate systems. The identity of the other cations in the material appears to have a distinct effect on the observed ^{6}Li chemical shift, and warrants future investigations. Arguments for a "first neighbor cation effect", resulting from both similar and dissimilar network modifiers, has previously been presented to explain variations in the ^{23}Na chemical shifts of silicate and aluminosilicate crystals.[31] Because of possible "first neighbor cation effects" observed above, only the ^{6}Li chemical shift versus shift parameter *A* correlations obtained for lithium phosphate crystals (Eqn 7), will be used in the analysis of ^{6}Li chemical shift variations in lithium phosphate glasses as described below.

4.2 *Lithium Ultraphosphate Glasses*

A linear increase in the ^{6}Li NMR chemical shift with increasing Li_2O concentration was observed for the ultraphosphate glasses (Figure 5a). The chemical shift varies from δ = -1.6 ppm for the $5Li_2O{\cdot}95P_2O_5$ glass to δ = –0.7 ppm for the $55Li_2O{\cdot}45P_2O_5$ glass. It is clear that there are no abrupt variations in the Li coordination environment with increasing Li_2O concentration. Even though T_g goes through a minimum at $x \sim 0.20$, no corresponding variation in the ^{6}Li chemical shift was observed. The variation of the chemical shift with NBO/P ratio (Eqn 2) is shown in Figure 6. There is a monotonic, but non-linear, increase in the chemical shift with decreasing network polymerization. This change reflects changes in the Li-O bonding environment due to increases in the average number of NBO available for coordination in the bulk material. Qualitative arguments about the variations of ^{6}Li chemical shift with the NBO/P ratio can be made, but no detailed structural information is obtainable from this type of analysis.

4.2.1 Determination of coordination number

At this point one of the more important structural parameters of these phosphate glasses, the CN of the lithium cation, has yet to be determined. In the previous section it was shown that the simple relationship between ^{6}Li chemical shift and CN[25] does *not* hold for crystalline lithium phosphate systems, precluding the use of that relationship for

determining CN in the analogous lithium phosphate glasses. Instead structural information, including CN, can be obtained from changes in the ^{6}Li chemical shift and the resulting average chemical shift parameter A relationship (Eqn 7). For the lithium phosphate glasses, increases in the Li_2O concentration produced a linear increase in A from ~1.0 to ~1.2 using the correlation in Eqn. 7. Inspection of Eqn 6 shows that this change in A is the function of three different structural parameters; oxygen bond valency, Li-O bond distance and CN. As a first approximation, one can assume that the total oxygen valency and the Li-O bond distances for all the oxygens in the summation can be replaced by an average value. Under these assumptions Eqn 6 can be rewritten as

$$\langle A \rangle \approx n \left\langle \frac{W}{r^3} \right\rangle \tag{9}$$

where n represents the average coordination number of the Li. This relationship assumes that due to the $1/r^3$ dependence the first coordination sphere of oxygen atoms dominates the interaction and the resulting value of the chemical shift parameter A. If the total oxygen bond valency is held constant (W = 2) for the entire Li_2O concentration range investigated, then the required variation of the Li-O bond distance as a function of Li_2O concentration for different Li CN can be evaluated from experimental values of A using Eqns 7 and 9 and is shown in Figure 8 (sloped lines with symbols). These curves represent the average Li-O bond distances that would be required to produce the observed chemical shift parameter A for the different Li CN.

These predicted Li-O bond distances are compared to the average lithium oxygen distance of 1.958 Å observed in crystalline $LiPO_3$ (unfilled circle in Figure 8). That value is approximately equally spaced between the predicted Li-O bond distance lines for CN = 4 and the CN = 5. The Li-O bond distance of 2.02 Å obtained from X-ray investigations of the binary $0.52Li_2O{\cdot}0.48P_2O_5$ glass system is also shown in Figure 8 (unfilled triangle). That Li-O bond distance corresponds closely to the predicted CN = 5 line, at the metaphosphate glass composition. Based on the assumptions in Eqn 9 these results suggest that the average Li CN is ~ 4 or 5 over the entire Li_2O concentration range investigated. A very short average Li-O bond distances (< 1.8 Å) for CN = 3, or a very

long average Li-O bond distances (>2.15Å) for CN = 6, would be required to explain the observed shift A values, suggesting that a Li CN of 3 and 6 are not present in the lithium ultraphosphate glasses. A Li CN =4 for the metaphosphate glass is consistent with the tetrahedral coordination reported in X-ray investigations of both the lithium metaphosphate crystal[35] and glass.[21]

If the Li CN is assumed to remain constant (CN ~ 4 or 5) then the increase in *A* with increasing Li_2O would result from a decrease in the average Li-O bond length. This decrease in the Li-O bond length is consistent with trends observed in Li_4SiO_4, where the average Li-O bond length decreases (plus a decrease in the average CN) with increasing values of *A* . This decrease in the Li-O bond length would also be consistent with the argument of increasing Li-O bond valency at higher Li_2O concentrations based on simple chemical shift trends. These trends of decreasing Li-O bond lengths with increasing *A* are not clearly apparent in the lithium phosphate crystals previously described (Table 1). Inspection of the average Li-O bond distances in the crystals reveals that there is a high degree of variability between the observed *A* and Li-O bond length. For example LT Li_3PO_4 has the longest average bond length of 1.976 Å and also the largest *A* value of 1.42. Similarly LiH_2PO_4 has a much shorter Li-O bond length of 1.956 Å and a correspondingly smaller *A* value of 1.32. The results for the $Li_4P_2O_7$ crystal include both the *A* values of 1.29 and 1.20 and corresponding average Li-O bond distances of 1.960 and 1.973 Å, respectively. These results demonstrates that the ^6Li chemical shift is a complex function of several different variables including CN, Li-O bond distance and total oxygen valency, and that attempts to correlate the observed chemical shift changes with a single variable will prove to be difficult.

4.2.2 Changes in the lithium environment

Given these observations an explanation for the T_g minimum at $x = 0.20$ mole fraction in the lithium phosphate glasses can be proposed. As noted in the discussion above the monotonic change of the lithium chemical shift with increasing Li_2O concentration (Figure 5a) precludes any dramatic changes in the average lithium environment as the cause for the T_g minimum. Instead, the observed minimum may result

from a balance between the effect of decreasing the number of P-O-P bonds in the network with increased Li_2O concentrations, against the influence of an increased number of O-Li-O bonds within the network. Hoppe has previously presented a structural model to describe packing densities in phosphate glasses.[42-44] In this model there are several composition intervals that describe the evolution of the glass structure. Initially the fully condensed P_2O_5 glass is composed entirely of Q^3 tetrahedra of which 40% of the oxygen atoms are terminal and the remaining fraction are bridging oxygens. As presented by Hoppe terminal oxygens represent double-bond oxygen (DBO) "defects" that can be removed by the addition of coordinating cations. For the Li phosphate glasses, there is a depolymerization of Q^3 tetrahedra to form Q^2 tetrahedra and corresponding non-bridging oxygens (NBO) as Li_2O is added. At low Li_2O concentrations, the Li cations will be isolated and are coordinated by both DBO and NBO. The NBO of the Q^2 groups are expected to coordinate with isolated Li-tetrahedra primarily through edge sharing, as depicted in Fig. 9a. As the Li_2O concentration increases the Li tetrahedra become less isolated and at some composition the Q^2 NBO must begin to be shared by different Li cations (corner sharing) as shown depicted in Fig 9b. The total number of terminal oxygens (TO) per Li cation (this includes both DBO and NBO oxygens) available for this coordination is defined by the ratio M_{TO}[42-44]

$$M_{TO} = \frac{1}{x} \tag{10}$$

where x is the mole fraction of Li_2O. As this ratio changes the local environment of the Li, and thus the ^6Li chemical shift, is expected to change as confirmed in Fig. 10. For M_{TO} ratios greater than the CN ($4 > M_{TO} > 25$) the variation of the ^6Li chemical shift is very small, suggesting that the Li environments do not vary within this composition range. This invariance would be expected for isolated LiO_n polyhedra as depicted in Fig. 9a.

The lowest Li_2O mole fraction at which all TO (including the DBO "defects") are coordinated to a Li, occurs when M_{TO} equals the lithium CN, and is simply defined by[42-44]

$$x = 1/CN \tag{11}$$

Equation 11 also represents the Li_2O concentration at which the preferential isolation of LiO_n polyhedra ends. As discussed above (and shown in Fig. 8) the average CN in the lithium ultraphosphate glasses is ~ 4 or 5, and so the critical Li_2O concentration ranges from $x \sim 0.20$ to 0.25. This is consistent with the observed mole fraction at the T_g minimum ($x \sim 0.2$).[10,11] For Li_2O concentrations above this critical mole fraction the LiO_n polyhedra are forced to link together by edges and corners (Fig. 9c), producing increased packing densities and the formation of cross-linking O-Li-O bridges between phosphate chains. This linking of LiO_n polyhedra, and the reduction of TO available to coordinate Li without sharing may produce the pronounced increase in the ^6Li chemical shift for M_{TO} ratios below 4 as observed in Fig. 10. The formation of bridging or cross-linking bonds at higher Li_2O concentrations is consistent with formation of more covalent Li-O bonds. Cross-linking or repolymerization via the formation of O-Li-O bonds has been previously proposed to explain the anomalous T_g behavior of ultraphosphate glasses.[10] This is consistent with Raman studies where a decrease in the $(P{=}O)_{sym}$ band frequencies reveals a delocalization of the π-bonding on the Q^3 tetrahedra with increasing Li_2O concentration. This delocalization would be predicted to increase network strength due to the formation of alkali-oxygen bridges.[11]

4.2.3 Distribution of lithium environment

The line width and apparent quadrupolar coupling can also be used to obtain qualitative information about the local structure in these glasses. As pointed out previously the ^7Li NMR line width is homogenously broadened by ^7Li-^7Li and ^7Li-^{31}P dipolar coupling giving rise to rather broad lines that are not easily interpreted.[28,29,45] For the less abundant ^6Li nuclei, the line broadening is inhomogenous in nature and reflects changes in the distribution of Li coordination environments. In general the ^6Li FWHM of the crystalline materials is smaller than the FWHM observed in the glasses, consistent with the expected increase in disorder for glasses. The gradual decrease in the ^6Li FWHM with Li_2O concentration for the lithium phosphate glasses (Fig. 5b and Table 2) suggests that there is a decrease in the distribution of Li environments as the metaphosphate composition is approached, and may reflect the increased formation of

more ordered linked LiO_4 or LiO_5 polyhedra. This trend is opposite to that observed in the ^7Li quadrupolar coupling constant which shows a small increase in the coupling constant with increasing Li_2O concentration, as a result of local disorder or a decrease in Li coordination symmetry as the glass approaches the metaphosphate composition. Also note that the magnitude of the quadrupolar coupling constant observed in the glasses (Table 2) is significantly lower than that observed in the corresponding lithium phosphate crystals (Table 1). This indicates that there is either an increase in the symmetry of the Li coordination, or that there is partial averaging of the quadrupolar interaction due to lithium diffusion at room temperature in the glasses. None of these trends correlate with the minimum observed for T_g at $x \sim 0.2$.

5. Conclusions

From these investigations of the ^6Li chemical shift in $xLi_2O{\cdot}(1\text{-}x)P_2O_5$ glasses only a monotonic variation of the local Li coordination with increasing Li_2O concentration is observed. These results suggest that the anomalous T_g behavior observed by Hudgens et al.[10,11] is not due to a major or abrupt change in the Li coordination environment, but instead result from continuous variations in the type of Li-O bonds being formed. At low Li_2O concentrations the network depolymerization due to breaking of P-O-P bonds with Li_2O addition is not sufficiently balanced by the formation of new Li-O bonds. This initial depolymerization is consistent with the observed decrease in the T_g at Li_2O concentration below $x = 0.20$. At the critical mole fraction ($x = 0.20$ - 0.25) repolymerization of the glass structure begins when the LiO_4 and LiO_5 polyhedra begin to link via sharing of edges, faces and vertices. The joining of polyhedra gives rise to O-Li-O cross-links or bridges between neighboring Q^2 tetrahedra producing an increase in the observed T_g. More detailed investigations of the changes in the Li-oxygen environment of ultraphosphate glasses using multidimensional techniques and ^{17}O NMR are presently being pursued.

Acknowledgements

Sandia is a multiprogram laboratory operated by Sandia Corporation, a Lockheed Martin Company, for the United States Department of Energy under Contract DE-AC04-94AL85000. The authors also thank Mark Rodrigez for access to the crystal analysis software and XRD analysis.

References

[1] J.A. Wilder J. Non-Cryst. Solids 38/39 (1980) 879.

[2] R.K. Brow, L. Kovacic, R.E. Loehman Ceram. Trans. 70 (1996) 177.

[3] M.J. Weber J. Non-Cryst. Solids 123 (1990) 208.

[4] D.E. Day, Z. Wu, C.S. Ray, P. Hrma J. Non-Cryst. Solids 241 (1998) 1.

[5] J. Fu J. Mater. Science 33 (1998) 1549.

[6] H. Hosono, F. Tsuchitani, K. Imai, Y. Abe, M. Maeda J. Mater. Res. 9 (1994) 755.

[7] A. Mogusmilankovic, M. Rajic, A. Drasner, R. Trojko, D.E. Day Phys. Chem. of Glasses 39 (1998) 70.

[8] T. Härig, G. Huber, I.A. Shcherbakov J. Appl. Phys. 52 (1981) 4450.

[9] J.W. Zwanziger Int. Review Phys. Chem. 17 (1998) 65.

[10] J.J. Hudgens, S.W. Martin J. Am. Ceram. Soc. 76 (1993) 1691.

[11] J.J. Hudgens, R.K. Brow, D.R. Tallant, S.W. Martin J. Non-Cryst. Solids 223 (1998) 21.

[12] S.W. Martin Eur. J. Solid State Inorg. Chem. 28 (1991) 163.

[13] R.J. Kirkpatrick, R.K. Brow Solid State Nuclear Magnetic Resonance 5 (1995) 9.

[14] R.K. Brow, R.J. Kirkpatrick, G.L. Turner J. Amer. Ceramic Society 76 (1993) 919.

[15] R.K. Brow, C.C. Phifer, G.L. Turner, R.J. Kirkpatrick J. Am. Ceram. Soc. 74 (1991) 1287.

[16] R.K. Brow, D.R. Tallant, J.J. Hudgens, S.W. Martin, A.D. Irwin J. of Non-Crystalline Solids 177 (1994) 221.

[17] T.M. Alam, R.K. Brow J. Non-Crystalline Solids 223 (1998) 1.

[18] M. Feike, C. Jager, H.W. Spiess J. Non-Cryst. Solids 223 (1998) 200.

[19] R.K. Sato, R.J. Kirkpatrick, R.K. Brow J. Non-Crystalline Solids 143 (1992) 257.

[20] E. Göbel, W. Müller-Warmuth, H. Olyschläger, H. Dutz J. Magn. Reson. 36 (1979) 371.

[21] K. Muruganandam, M. Seshasayee, S. Patnaik Solid State Ionics 89 (1996) 313.

[22] Preliminary results of the Li NMR investigations appear in the International Conference on Glasses (ICG) proceedings(1998).

[23] C. Keffer, A. Mighell, F. Mauer, H. Swanson, S. Block Inorg. Chem. 6 (1967) 119.

[24] H. Günther *High-resolution ^{6,7}Li NMR of Organolithium Compounds*; H. Günther, Ed.; John Wiley & Sons: New York, NY, 1996, pp 376.

[25] Z. Xu, J.F. Stebbins Solid State Nuclear Magnetic Resonance 5 (1995) 103.

[26] A. Abragam *Principles of Nuclear Magnetism*; Oxford University Press: New York, NY, 1961.

[27] C.P. Slichter *Principles of Magnetic Resonance*; 3rd ed.; Springer-Verlag: New York, NY, 1989.

[28] W. Müller-Warmuth, H. Eckert Phys. Reports 88 (1982) 91.

[29] H. Eckert, Z. Zhang, J.H. Kennedy Mat. Res. Soc. Symp. Proc. 135 (1989) 259.

[30] P.S. Fiske, J.F. Stebbins Amer. Miner. 79 (1994) 848.

[31] X. Xue, J.F. Stebbins Phys. Chem. Minerals 20 (1993) 297.

[32] H. Koller, G. Engelhardt, A.P.M. Kentegens, J. Sauer J. Phys. Chem. 98 (1994) 1544.

[33] V.J. Zeeman Acta Cryst. 13 (1960) 863.

[34] O.V. Yakubovich, O.K. Melnikov Kristallografiva 39 (1994) 815.

[35] P.J.C. Guitel, I. Tordjman Acta Cryst. B32 (1978) 2960.

[36] The ratio NBO/P used here is equivalent to the NBO/T described by Xue and Stebbins, Ref 31.

[37] N.E. Brese, M. O'Keefee Acta Cryst. B47 (1991) 192.

[38] I.D. Brown, D. Altermatt Acta Cryst. B41 (1985) 244.

[39] I.D. Brown, R.D. Shannon Acta Cryst. A29 (1973) 266.

[40] B.H.W.S. De Jong, D. Ellerbroek, A.L. Spek Acta Cryst. B50 (1994) 511.

[41] The spectra in Fig. 4 of Ref. 25 for Li_4SiO_4 was deconvoluted to give four resonances $\delta = 1.6$ (23%), $\delta = 0.9$ (52%), $\delta = 0.4$ (9%) and $\delta = 0.75$ (16%). These chemical shifts and relative areas differ from those reported in Ref. 25, but the relative areas correspond nicely to the different coordination environments reported in the crystal structure (Ref. 40). For the multiple Li environments average *A* values based on the observed relative concentrations are reported.

[42] U. Hoppe J. Non-Cryst. Solids 195 (1996) 138.

[43] U. Hoppe, G. Walter, D. Stachel, A. Barz, A.C. Hannon Z. Naturforsch. 52a (1997) 259.

[44] U. Hoppe, G. Walter, R. Kranold, D. Stachel, A. Barz J. Non-Cryst. Solids 192&193 (1995) 28.

[45] H. Eckert Progress in NMR Spectroscopy 24 (1992) 159.

Figure 1: Variation of the glass transition temperature (T_g) with Li_2O mole fraction in the $xLi_2O{\cdot}(1\text{-}x)P_2O_5$ glasses. A minimum in T_g is observed near $x \sim 0.2$. Adapted from Ref. [10,11].

Figure 2: The natural abundance a) ^7Li and b) ^6Li MAS NMR spectra for crystalline Li_3PO_4, low temperature (LT) form. The ^7Li spectra shows a strong central resonance for the $\pm 1/2 \leftrightarrow \mp 1/2$ transition and a spinning sideband manifold resulting from the $\pm 3/2 \leftrightarrow \pm 1/2$ transitions. The ^6Li spectra reveals only a single isotropic resonance, with a negligible second order quadrupolar shift, providing a good approximation of the true chemical shift.

Figure 3: The natural abundance ^6Li MAS NMR spectrum for crystalline a) $Li_4P_2O_7$ and b) $LiPO_3$. In $Li_4P_2O_7$ the four inequivalent Li sites in the unit cell give rise to two resolvable resonances, while in $LiPO_3$ ten iequivalent Li sites in the unit cell give rise to 4 resolvable ^6Li NMR resonances. The simulated spectra and individual line components are shown below the experimental spectra.

Figure 4: Natural abundance a) ^7Li and b) ^6Li MAS NMR spectra for the metaphosphate $xLi_2O{\bullet}(1\text{-}x)P_2O_5$ glass ($x = 0.5$). Similar spectra were obtained for the entire range range of x investigated. The observed ^6Li chemical shift and line widths (Table 2) were utilized in describing the local Li coordination environment, as detailed in the text.

Figure 5: The variation of the a) ^6Li NMR chemical shift and b) FWHM line width with Li_2O concentrations. A linear increase in the Li chemical shift with increasing Li_2O

concentration is observed, while a general decrease in the Li FWHM with increasing Li_2O concentration is observed.

Figure 6: The variation of the ^6Li NMR chemical shift with the ratio of non-bonding oxygens per phosphorous tetrahedra (NBO/P). The results for the crystalline samples listed in Table 1 are shown: $LiPO_3$ (♦,◇) $Li_4P_2O_7$ (■,❑), Li_3PO_4 (LTF) (▼), Li_3PO_4(HTF) (●) and LiH_2PO_4 (▲). For those crystals with multiple resolved ^6Li chemical shifts, unfilled symbols are for individual chemical shifts and the filled symbols represent the weigthed average chemical shift. The experimental results for the $xLi_2O•(1-x)P_2O_5$ glass series is denoted by (○).

Figure 7: Correlations between the observed ^6Li NMR chemical shift and the chemical shift parameter *A* (defined by Eqn 6). The results for the lithium phosphate crystals listed in Table 1 are given by (●) and for the lithium silicate Li_4SiO_4 crystal by (○). The difference in slope suggest that there are nearest neighbor cation effects influencing the observed ^6Li chemical shift.

Figure 8: The predicted variation of the Li-O bond distance versus Li_2O concentration, from Eqns 7 and 9 and the experimental chemical shifts, for the $xLi_2O•(1-x)P_2O_5$ glass series at different Li coordination numbers (CN); CN = 6 (▲). CN = 5 (■), CN = 4 (●) and CN = 3 (▼) The average Li-O bond distance observed in crystalline $LiPO_3$ (○) and the the binary $0.52Li_2O·0.48P_2O_5$ glass (▽) are shown for comparison. Details of the analysis is given in the text.

Figure 9: A schematic illstration of the network structures of binary lithium ultraphosphate glasses corresponding to different Li_2O concentration: a) low, b) mid and c) high.

Figure 10: Variation of the ^6Li NMR chemical shift with the ratio of terminal oxygens per Li atom (M_{TO}) in the $xLi_2O\bullet(1\text{-}x)P_2O_5$ glass series. The critical Li_2O concentration is predicted to occur when M_{TO} equals the Li coordination number and is denoted by hashed region.

Table 1

Solid state ^{6}Li and ^{7}Li MAS NMR chemical shifts and line widths for selected crystalline lithium phosphates.

Composition	PDF[a]	^{7}Li δ (ppm)[b]	^{7}Li FWHM (Hz)[c]	^{7}Li C_q (kHz)[d]	^{6}Li δ (ppm)[b]	^{6}Li FWHM (Hz)[c]	CN[e]	$\langle A \rangle$[f]
Li_3PO_4 (LT)[g]	25-1030	0.2 ± 0.2	943	110	0.32 ± 0.05	34	4	1.42
Li_3PO_4(HT)[g]	15-0760	0.2 ± 0.2	1020	120	0.36 ± 0.05	30	4	1.38
LiH_2PO_4	21-0498	-0.3±0.2	400	80	-0.26 ± 0.05	22	4	1.32
$Li_4P_2O_7$	13-0440	-0.4 ± 0.2	731	150	-0.23 ± 0.05	40	4	1.29
					-0.78 ± 0.05	46	4	1.20
$LiPO_3$	26-1177	-0.5 ± 0.2	757	110	0.16 ± 0.05	23	4	1.41
					-0.14± 0.05	25	4	1.39
					-0.43 ± 0.05	37	4	1.25
					-1.15 ± 0.05	32	4	1.09

[a] Powder diffraction file (PDF) number for respective crystal. [b] Observed chemical shift with respect to external 1M aqueous LiCl standard (δ = 0.0 ppm). [c] Full width at half maximum (FWHM) line width. [d] Quadrupolar coupling constant $C_q = e^2qQ/h$ estimated from width of spinning sideband manifold. [e] lithium coordination number from published crystal structures. [f] Average chemical shift parameter defined in eqn 6. [g] Low temperature (LT) and high temperature (HT) form of Li_3PO_4.

Table 2
Solid state ^{6}Li and ^{7}Li MAS NMR chemical shifts and line widths for various $xLi_2O \cdot (1\text{-}x)P_2O_5$ glasses

Glass	^{7}Li δ (ppm)[a]	^{7}Li FWHM (Hz)[b]	^{7}Li C_q (kHz)[c]	^{6}Li δ (ppm)[a]	^{6}Li FWHM (Hz)[b]
$0.05Li_2O{\cdot}0.95P_2O_5$	-1.5 ± 0.2	249	100	-1.50 ± 0.05	55
$0.10Li_2O{\cdot}0.90P_2O_5$	-1.5 ± 0.2	240	130	-1.40 ± 0.05	56
$0.15Li_2O{\cdot}0.85P_2O_5$	-1.4 ± 0.2	214	140	-1.33 ± 0.05	51
$0.20Li_2O{\cdot}0.80P_2O_5$	-1.3 ± 0.2	281	150	-1.25 ± 0.05	58
$0.25Li_2O{\cdot}0.75P_2O_5$	-1.3 ± 0.2	307	175	-1.15 ± 0.05	46
$0.35Li_2O{\cdot}0.65P_2O_5$	-1.0 ± 0.2	466	200	-1.03 ± 0.05	52
$0.43Li_2O{\cdot}0.57P_2O_5$	-0.9 ± 0.2	519	210	-0.87 ±0.05	41
$0.50Li_2O{\cdot}0.50P_2O_5$	-0.9 ± 0.2	569	210	-0.80 ± 0.05	41
$0.55Li_2O{\cdot}0.45P_2O_5$	-0.7 ± 0.2	575	215	-0.64 ± 0.05	43

[a] Observed chemical shift with respect to external 1M LiCl (δ = 0.0 ppm).[b] Full width at half maximum (FWHM) line width. [c] Quadrupolar coupling constant $C_q = e^2qQ/h$ Estimated from width of spinning sideband manifold.

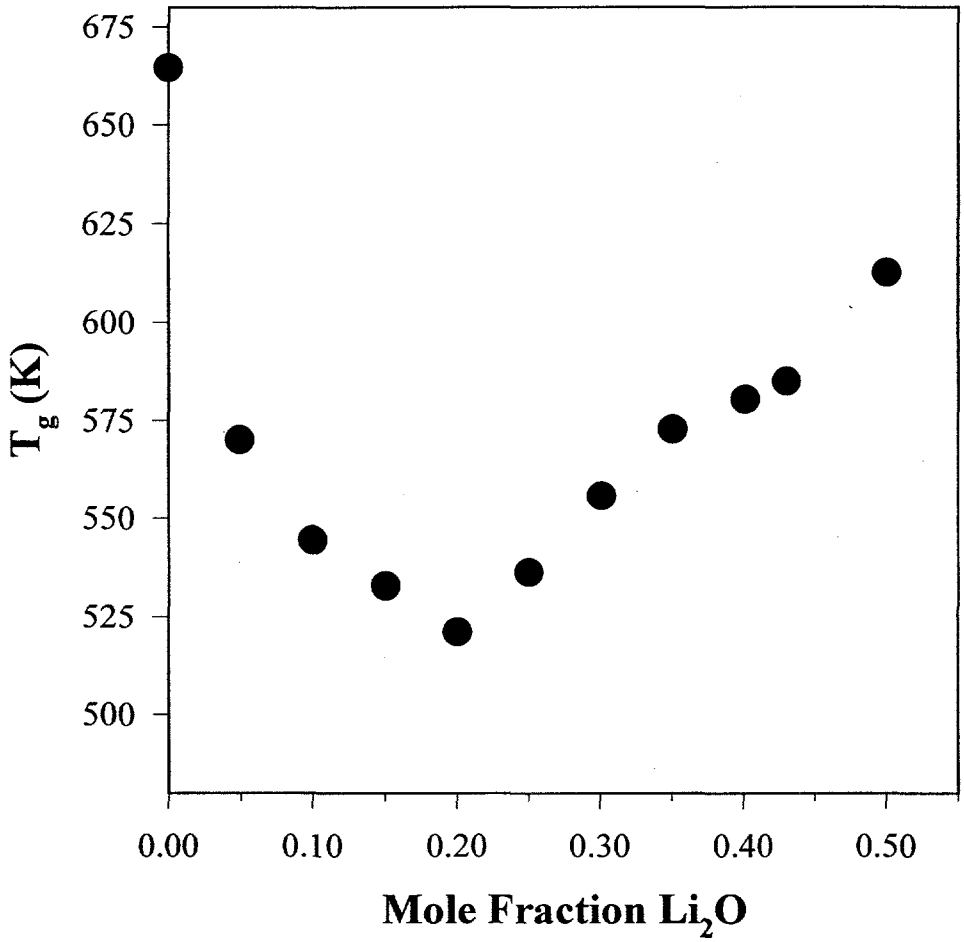

Alam et al. Fig. 1

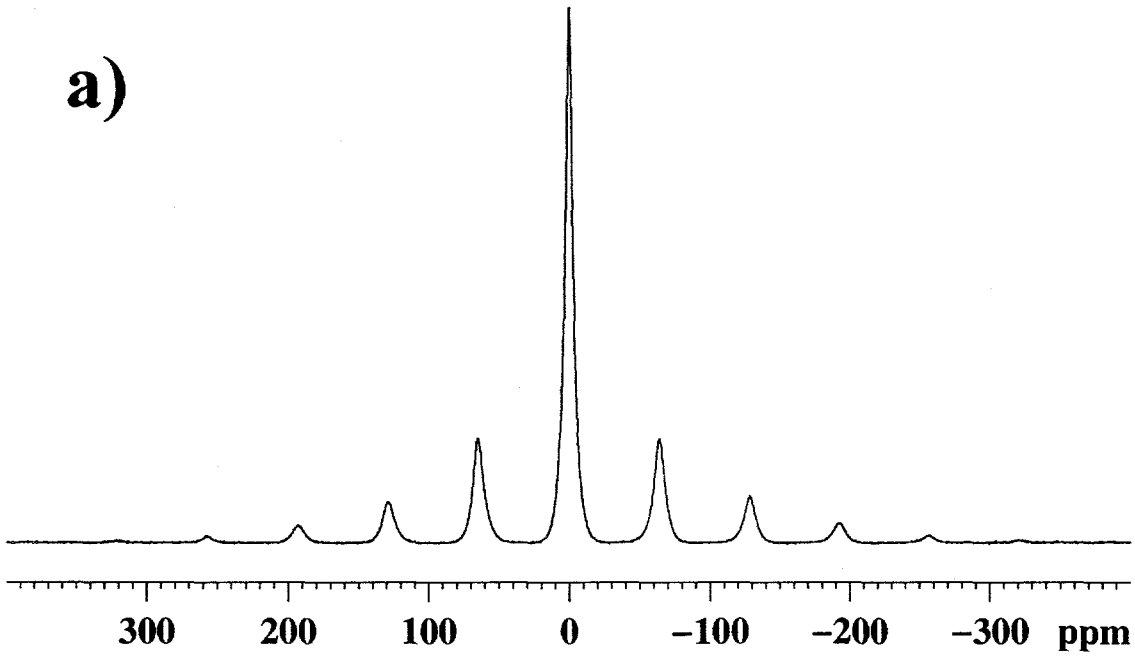

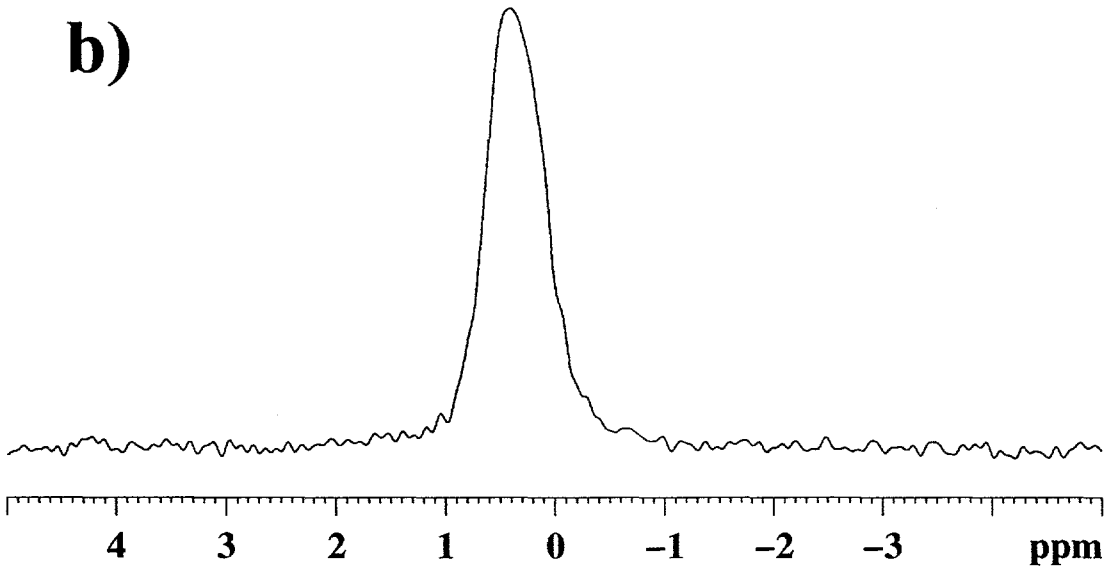

Alam et al. Fig. 2

Alam Fig 3

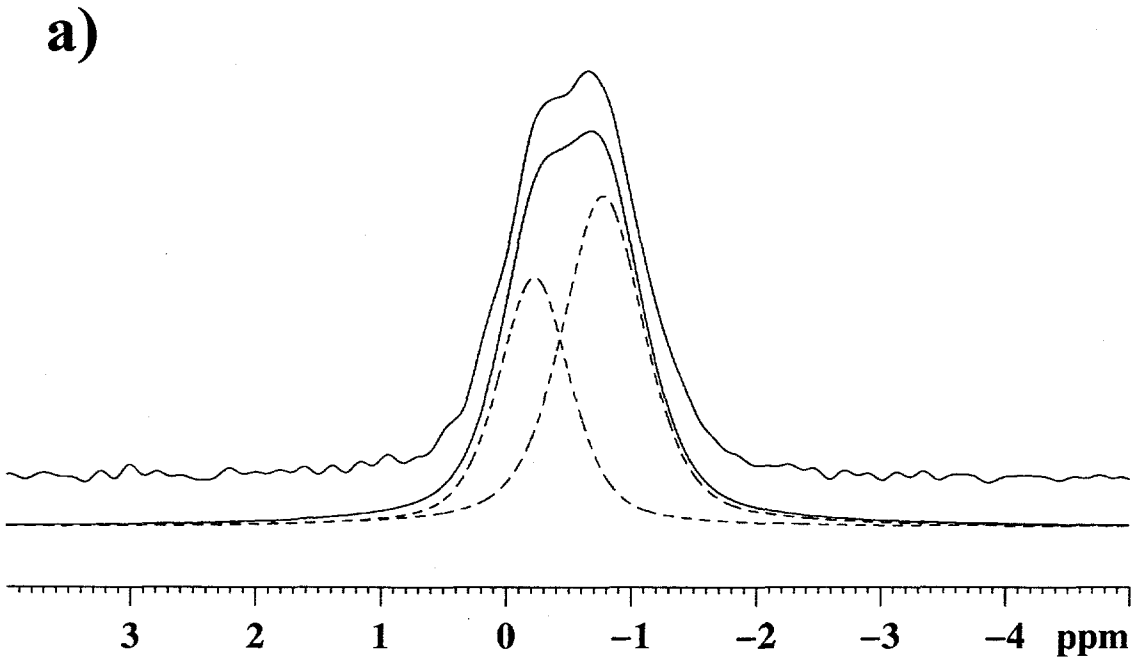

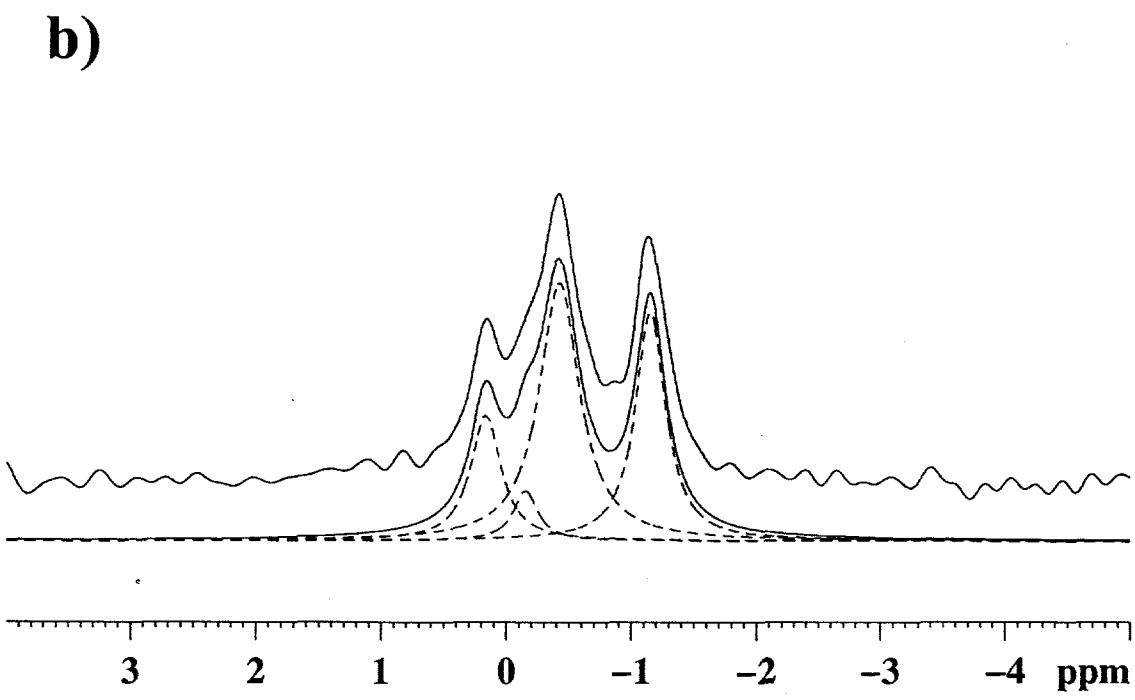

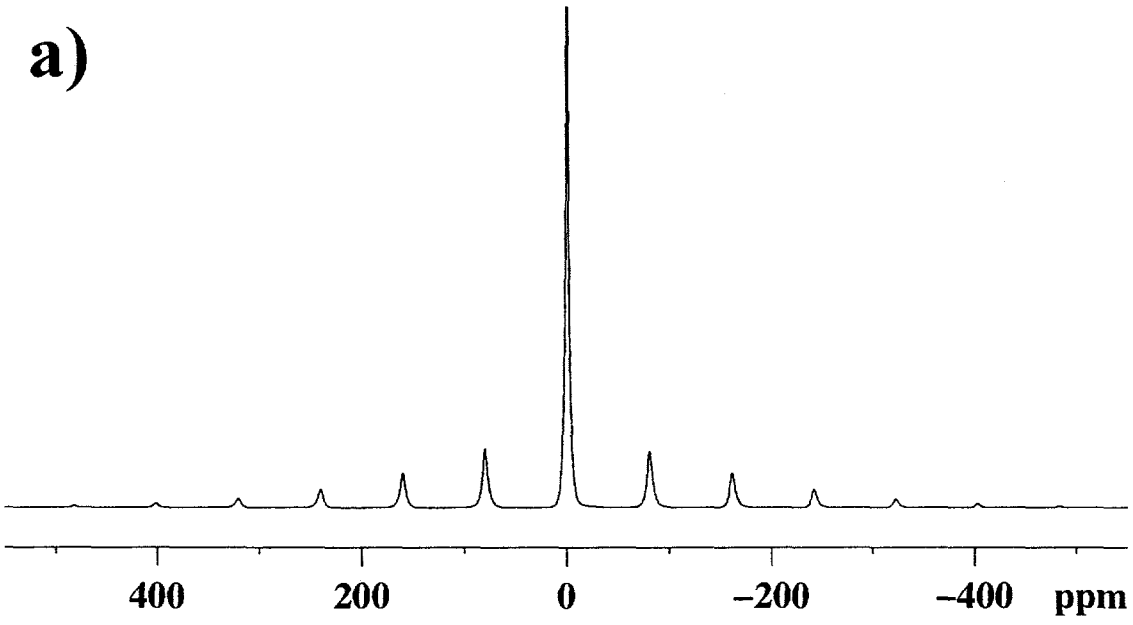

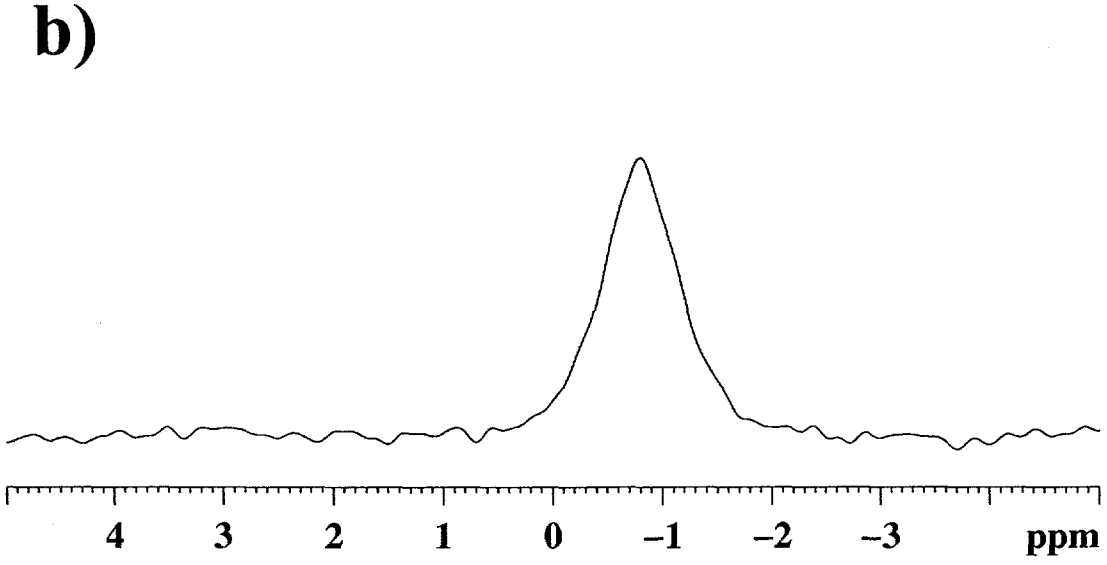

Alam et al. Fig. 4

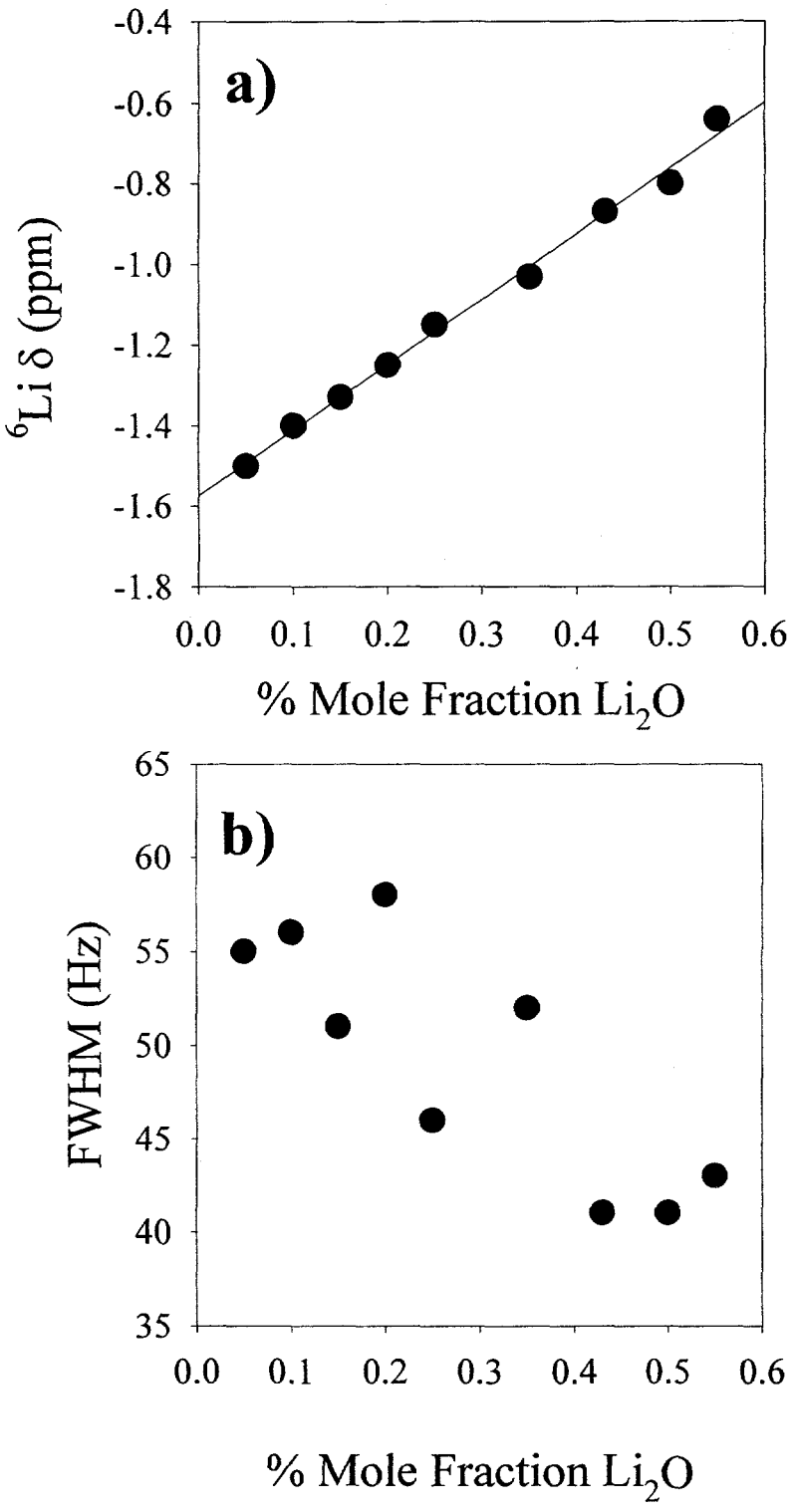
a)
-0.4
-0.6
-0.8
-1.0
-1.2
-1.4
-1.6
-1.8
^{6}Li δ (ppm)
0.0
0.1
0.2
0.3
0.4
0.5
0.6
% Mole Fraction Li_2O
b)
65
60
55
50
45
40
35
FWHM (Hz)
0.0
0.1
0.2
0.3
0.4
0.5
0.6
% Mole Fraction Li_2O

Figure 5

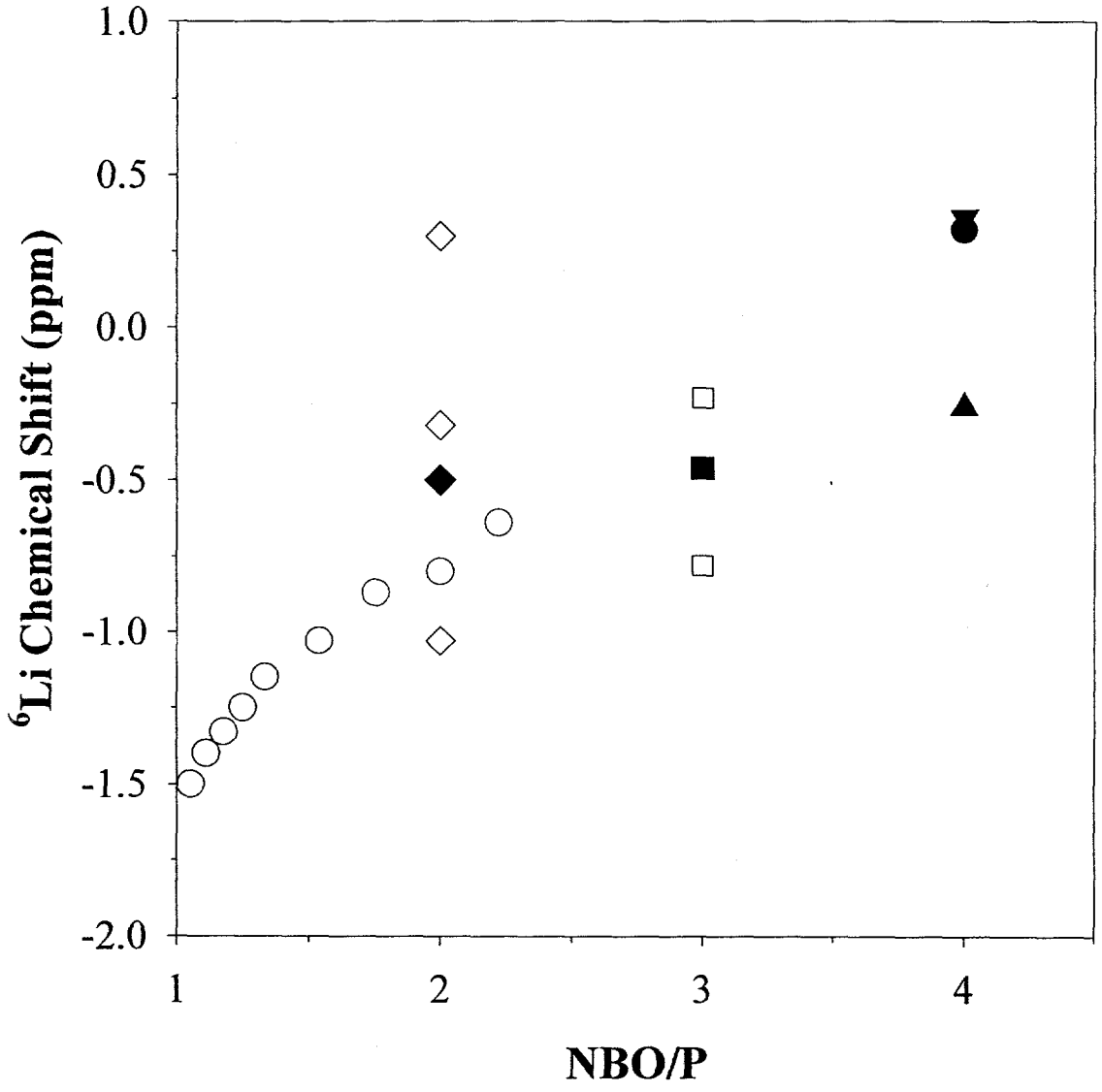

Figure 6

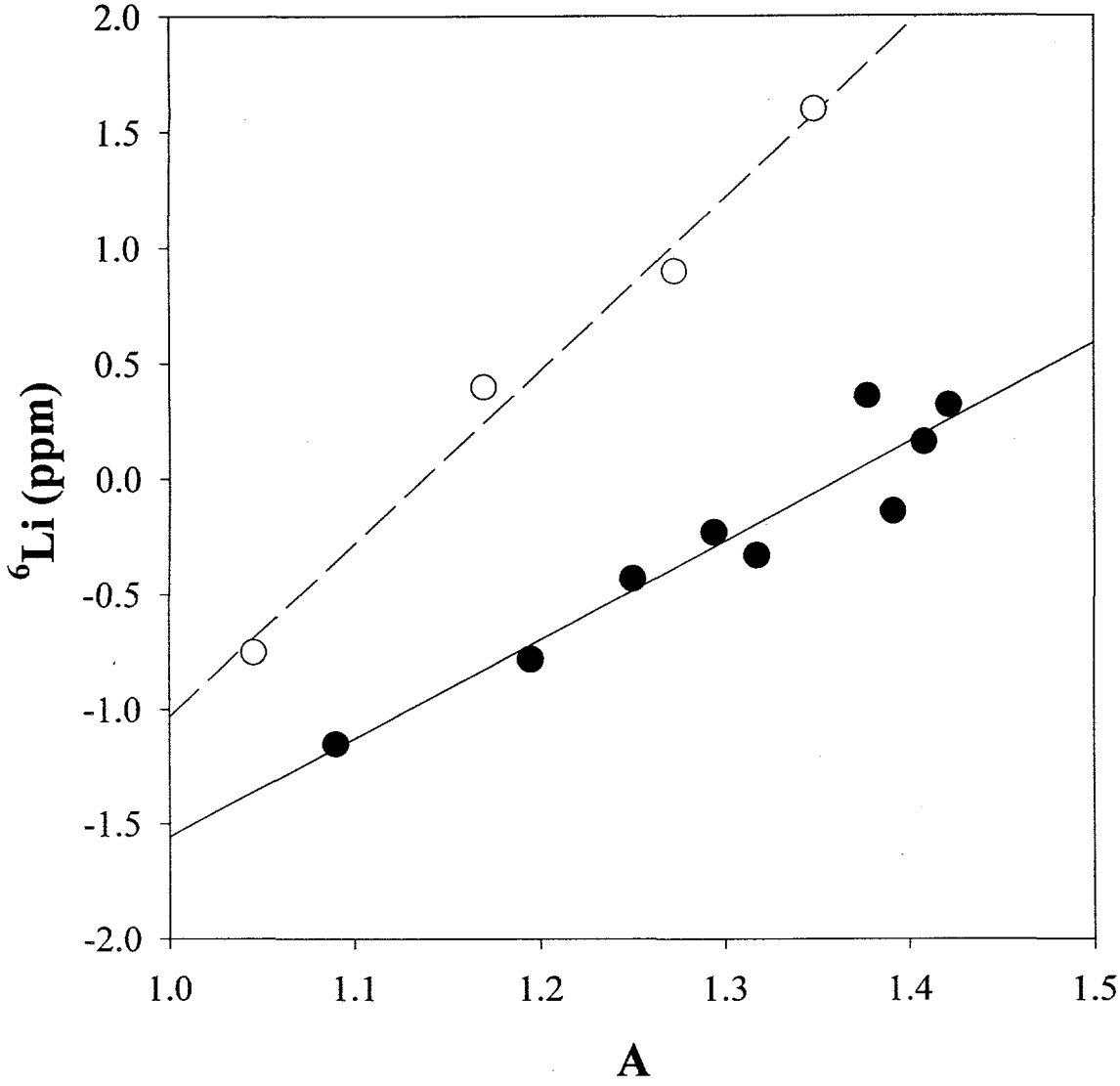

Figure 7

Figure 8

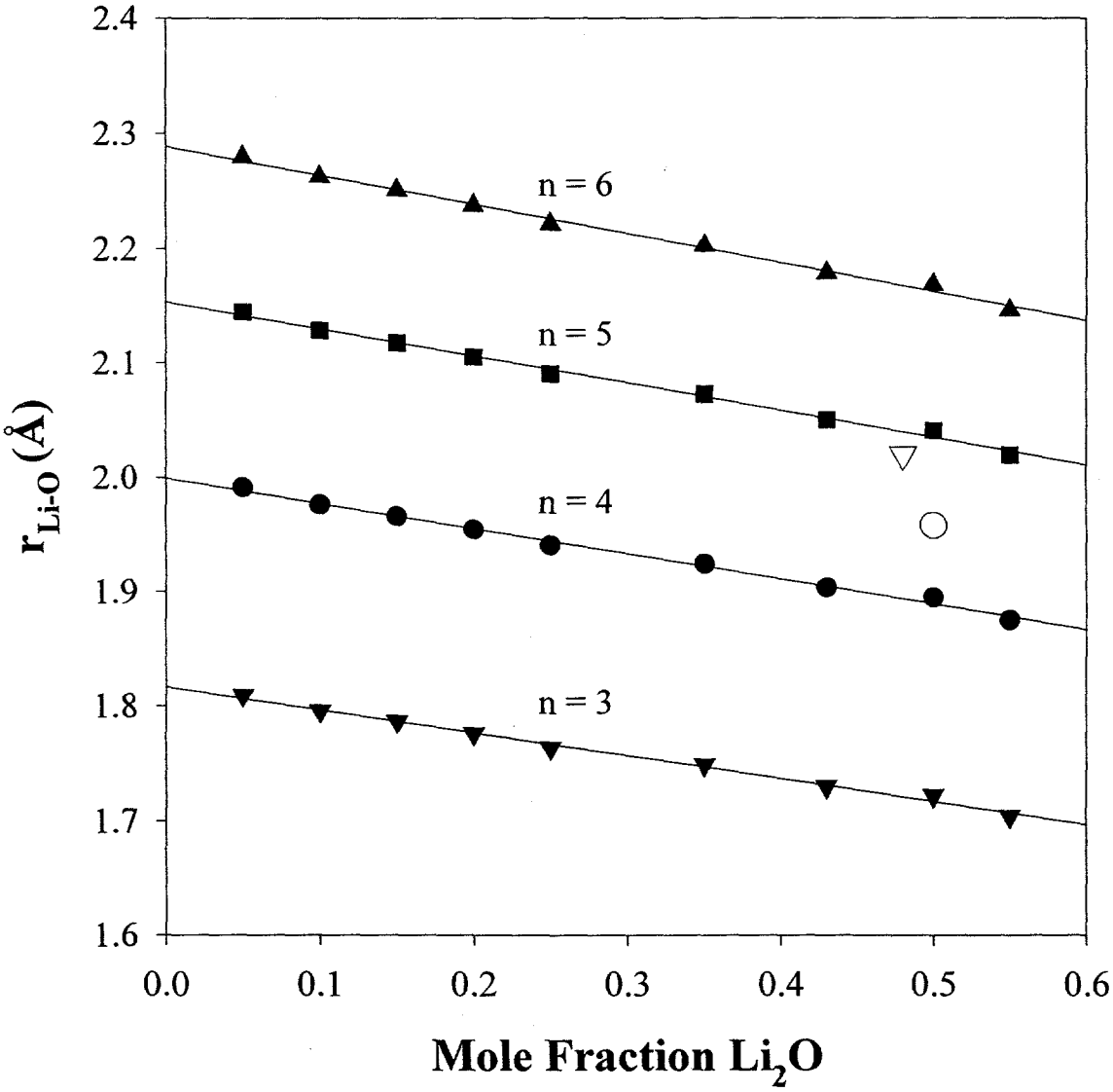
2.4
2.3
2.2
2.1
2.0
1.9
1.8
1.7
1.6
n = 6
n = 5
n = 4
n = 3
r_{Li-O} (Å)
0.0
0.1
0.2
0.3
0.4
0.5
0.6
Mole Fraction Li_2O

a)

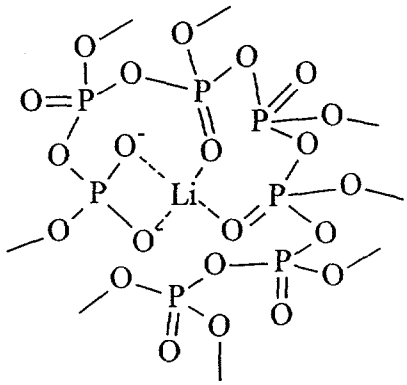

b)

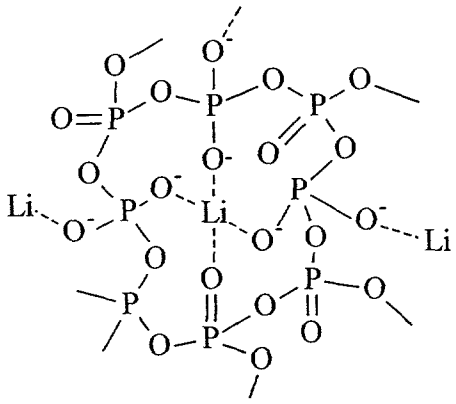

c)

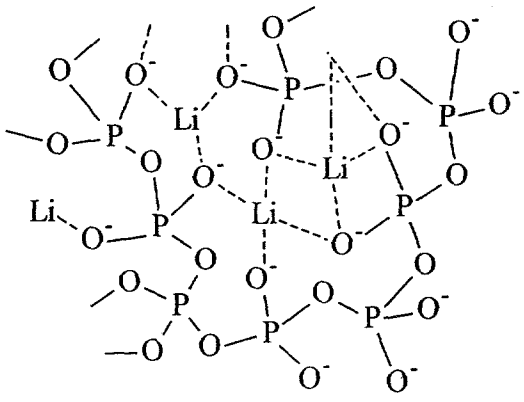

Figure 9 Alam

Alam Fig. 10

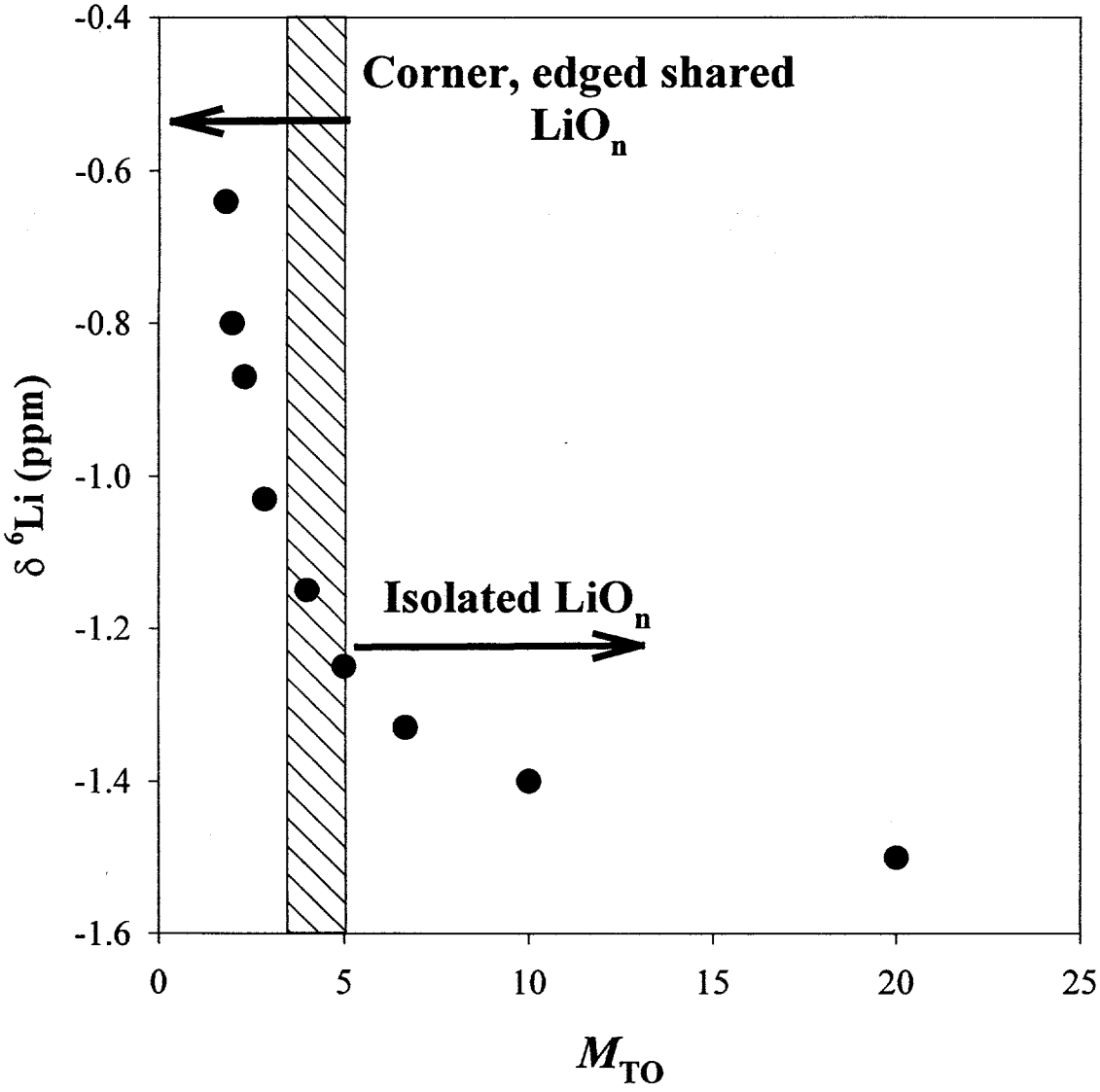
Corner, edged shared
LiO$_n$
Isolated LiO$_n$
δ ^{6}Li (ppm)
-0.4
-0.6
-0.8
-1.0
-1.2
-1.4
-1.6
0
5
10
15
20
25
M_{TO}